Theory of Nonequilibrium Coherent Transport through an Interacting Mesoscopic Region Weakly Coupled to Electrodes

Yu Zhu and Tsung-han Lin*

State Key Laboratory for Mesoscopic Physics and

Department of Physics, Peking University, Beijing

100871, China

Qing-feng Sun

Center for the Physics of Materials and

Department of Physics, McGill University, Montreal,

PQ, Canada H3A 2T8

()

Abstract

We develop a theory for the nonequilibrium coherent transport through a mesoscopic region, based on the nonequilibrium Green function technique. The theory requires the weak coupling between the central mesoscopic region and the multiple electrodes connected to it, but allows arbitrary hopping and interaction in the central region. An equation determining the nonequilibrium distribution in the central interacting region is derived and plays an important role in the theory. The theory is applied to two special cases for demonstrations, revealing the novel effects associated with the combination of phase coherence, Coulomb interaction, and nonequilibrium distribution.

PACS numbers: 73.63.Kv, 85.35.Ds, 73.23.Hk, 73.40.Gk.

In the realm of mesoscopic transport, the basic rules of the traditional electronics breakdown. When the size of device is smaller than the electron mean free path in the material, electrons will behave like a wave rather than particles. Meanwhile, with the reduced size of device, the Coulomb interaction among electrons becomes important. An additional electron has to overcome the repulsion from other electrons in the device before entering it. Moreover, due to lack of inelastic collisions, the thermal distribution in the device is no longer a equilibrium one when electrodes are biased with finite voltages. Therefore, a theory containing the above three "ingredients"—phase coherence, Coulomb interaction, and nonequilibrium—is of particular interest in the mesoscopic transport.

Using nonequilibrium Keldysh formalism, Meir *et al.* derived a formula, in which the current flowing out of an electrode is expressed in term of the Green functions of the central region [1]. The remaining task is to find out these Green functions. Unfortunately, there seems no standard method to derive them, although various approximation schemes were used for special problem in specific system, e.g., large-N expansion [2], truncation for equation of motion [3], introducing an interpolative self-energy [4], Ng's ansatz for lesser self-energy [5], etc. In fact, too much physics is hidden in the general Hamiltonian, and it is hopeless to invent a theory covering everything. If we restrict ourselves to the weak coupling case, the complex Kondo physics will be ruled out. In these circumstances, the Green functions in the "atomic limit" should be a good starting point for the construction of the full Green functions, and we shall show that a general solution to the problem is possible. We note that similar idea has been addressed in the linear response theory by several authors [6,7], but hardly investigated in the nonlinear regime [8].

The aim of this paper is to present a scheme for the calculation of the Green functions, and hence establish a theory of nonequilibrium coherent transport through an interacting mesoscopic region. As a price, the coupling between the central mesoscopic region and the electrodes is required to be relatively small. Electron transport through the mesoscopic region is viewed as a summation over various coherent processes via many-body quantum states, weighted by nonequilibrium thermal probabilities. The many-body quantum states in the central region can be found by exact diagonalization, while the nonequilibrium distribution can be determined by an equation derived in the text .

The mesoscopic system under consideration is modelled by the Hamiltonian (hereafter $e = \hbar = 1$), $H = H_{cent} + \sum_\beta H_\beta + H_T$, where $H_{cent} = H_{cent}(\{c_i\}, \{c_i^\dagger\})$ is a general Hamiltonian for the central region with M-sites (spin index has been absorbed into the

site index i), $H_\beta = \sum_\beta (\epsilon_k - V_\beta) a^\dagger_{\beta k} a_{\beta k}$ is the Hamiltonian for the βth electrodes, and $H_T = \sum_{\beta k i} \left[v_{\beta i} a^\dagger_{\beta k} c_i + H.c. \right]$ is the tunnel coupling between them. This Hamiltonian is applicable to a large variety of mesoscopic systems, such as molecular devices, tunneling coupled carbon nanotubes, quantum dot arrays, Aharonov-Bohm rings embedded with quantum dots, etc.

Define the Green function of the central region and the self-energy arise from the coupling with βth electrodes as $\mathbf{G}^{r,a,<}_{ij}(t_1,t_2) \equiv \langle\langle c_i(t_1)|c^\dagger_j(t_2)\rangle\rangle^{r,a,<}$ and $\mathbf{\Sigma}^{r,a,<}_{\beta,ij}(t_1,t_2) \equiv \sum_k v^*_{\beta i} \langle\langle a_{\beta k}(t_1)|a^\dagger_{\beta k}(t_2)\rangle\rangle^{r,a,<}_0 v_{\beta j}$, where the superscript $r,a,<$ denote for the retarded, advanced, lesser Green function and self-energy, respectively; the subscript 0 denotes for the Green function in the decoupling limit. Following Meir *et al.*, the current flowing out of the βth electrodes can be expressed in the compact form $I_\beta = \int \frac{d\omega}{2\pi} Tr \left\{ 2\,\mathrm{Re}\left[\mathbf{G}(\omega)\mathbf{\Sigma}_\beta(\omega)\right]^< \right\}$, where $[AB]^< \equiv A^r B^< + A^< B^a$, $\mathbf{G}^{r,a,<}(\omega)$ and $\mathbf{\Sigma}^{r,a,<}(\omega)$ are the Fourier transformed Green function and self-energy. In the wide bandwidth limit, the self-energy can be evaluated as $\mathbf{\Sigma}^r_\beta(\omega) = -\frac{\mathrm{i}}{2}\mathbf{\Gamma}_\beta$ and $\mathbf{\Sigma}^<_\beta(\omega) = \mathrm{i} f_\beta(\omega)\mathbf{\Gamma}_\beta$, where $\mathbf{\Gamma}_{\beta,ij} \equiv 2\pi D_\beta v^*_{\beta i} v_{\beta j}$ with D_β being the density of states at the Fermi surface of the βth electrode, $f_\beta(\omega) \equiv f(\omega - V_\beta)$ with $f(\omega)$ being the Fermi distribution function. We assume that the coupling between the central region and the electrodes is relatively small, i.e., $\Gamma_{\beta,ij} \ll k_B T$. Under this assumption, the Green function of the central region can *approximately* be written in a Dyson equation form $\mathbf{G} = \tilde{\mathbf{g}} + \tilde{\mathbf{g}}\mathbf{\Sigma}_0\mathbf{G}$, with $\tilde{\mathbf{g}} \equiv \lim_{H_T \to 0} \mathbf{G}$ being the Green function in the decoupling limit, $\mathbf{\Sigma}_0 \equiv \sum_\beta (\mathbf{\Sigma}_\beta)$ being the self-energy contributed by the coupling with electrodes. (This approximation is amount to a proper truncation of equation of motion.) Accordingly, the approximate "Dyson equation" for $\mathbf{G}^r$ and the "Keldysh equation" for $\mathbf{G}^<$ are

$$\mathbf{G}^r = \tilde{\mathbf{g}}^r + \tilde{\mathbf{g}}^r \mathbf{\Sigma}^r_0 \mathbf{G}^r \ , \tag{1}$$

$$\mathbf{G}^< = \mathbf{G}^r \mathbf{\Sigma}^<_0 \mathbf{G}^a \ . \tag{2}$$

Consequently, the current formula can be rewritten in a Landauer type as if in the noninteracting case [1],

$$I_\beta = \sum_{\alpha \neq \beta} \int \frac{d\omega}{2\pi} T_{\alpha\beta}(\omega) \left[f_\beta(\omega) - f_\alpha(\omega) \right] \ , \tag{3}$$

with $T_{\alpha\beta}(\omega) \equiv Tr \mathbf{G}^r \mathbf{\Gamma}_\alpha \mathbf{G}^a \mathbf{\Gamma}_\beta$.

The remaining task is to calculate the retarded Green function in the decoupling limit. It is straightforward to exactly diagonalize $H_{cent}(\{c_i\}, \{c^\dagger_i\})$ in the particle occupation bases $\{(c^\dagger_M)^{N_M} \cdots (c^\dagger_2)^{N_2} (c^\dagger_1)^{N_1} |0\rangle$ where $N_i = 0$ or 1, and obtain the 2^M eigenstates $\{E_n, |n\rangle\}$.

Once again, under the weak coupling assumption, the density matrix operator of the central region is supposed to have the *diagonal* form $\rho_{cent} = \sum_n P_n |n\rangle \langle n|$, with the constraint $\sum_n P_n = 1$. Here, the central region is regarded as "system", while the electrodes are "environment" in local equilibrium. Given $\{P_n\}$, the decoupled Green functions can be expressed as

$$\langle\langle A|B\rangle\rangle_0^r = \sum_{nm} \frac{P_n + P_m}{\omega - (E_n - E_m) + \mathrm{i}0^+} \langle m|A|n\rangle \langle n|B|m\rangle \quad , \tag{4}$$

$$\langle\langle A|B\rangle\rangle_0^< = \sum_{nm} 2\pi\mathrm{i}\ P_n \delta\left[\omega - (E_n - E_m)\right] \langle m|A|n\rangle \langle n|B|m\rangle \quad , \tag{5}$$

where A and B are operators composed of $\{c_i\}$ and $\{c_i^\dagger\}$. So the determination of the nonequilibrium distribution $\{P_n\}$ lies in the heart of the theory. In the linear response regime, i.e., $|V_\beta - V_{\beta'}| \ll k_B T$ and hence $V_\beta \approx V_0$, the central region is in a thermal equilibrium, and the distribution can be written as $P_n = \frac{1}{Z} e^{-(E_n - N_n V_0)/k_B T}$. For the case of nonequilibrium, however, $\{P_n\}$ is determined by the coupling to electrodes with different chemical potentials, and in principle needs a self-consistent calculation. Our strategy is to choose a proper set of observables $\{O\}$ and establish the equations of $\{P_n\}$ by the *stationary* condition

$$\langle \partial_t O\rangle = \langle \mathrm{i}\,[H, O]\rangle = 0 \ . \tag{6}$$

We point out that the 2^M conservables $\{O_l \equiv |l\rangle \langle l|\}$ ($|l\rangle$ is the eigenstate of H_{cent}) are ideal candidates for the task. Notice that

$$\langle \mathrm{i}\,[H, O_l]\rangle = 2\,\mathrm{Re} \int \frac{d\omega}{2\pi} \sum_{\beta k} \sum_{ij} \left[\langle\langle [c_i, O_l]|c_j^\dagger\rangle\rangle v_{\beta j}^* \langle\langle a_{\beta k}|a_{\beta k}^\dagger\rangle\rangle_0 v_{\beta i}\right]^< \quad , \tag{7}$$

and make the approximation $\langle\langle [c_i, O_l]|c_j^\dagger\rangle\rangle \approx \langle\langle [c_i, O_l]|c_j^\dagger\rangle\rangle_0$ under the weak coupling approximation, one can derive a set of equations of $\{P_n\}$ as

$$\sum_\beta \sum_{nm} \left[P_m f_\beta(E_n - E_m) - P_n \bar{f}_\beta(E_n - E_m)\right] \tilde{\Gamma}_{nm}^\beta Q_{nm}^l = 0 \quad (l = 1, 2 \cdots 2^M) \ , \tag{8}$$

where n and m run over all the eigenstates of H_{cent}, $\tilde{\Gamma}_{nm}^\beta \equiv \sum_{ij} \langle m|c_i|n\rangle \langle n|c_j^\dagger|m\rangle \Gamma_{\beta,ij}$, $Q_{nm}^l \equiv \delta_{nl} - \delta_{ml}$, and $\bar{f}_\beta(\omega) \equiv 1 - f_\beta(\omega)$. Because $\sum_l |l\rangle \langle l| = 1$, the 2^M conservables can produce 2^M-1 independent equations, and the constraint $\sum_n P_n = 1$ should be supplemented for completeness. Eq.(8) is the central result of this work, which determines the nonequilibrium distribution in an interacting system. With $\{P_n\}$ solved from the set of equations, one can calculate both nonequilibrium tunneling current and various quantities of the central region.

To sum up, Eq.(1), (3), (4), and (8) consist of the frame for the calculation of the nonequilibrium coherent transport through an interacting mesoscopic region, requiring weak coupling between the central region and the electrodes, but allowing arbitrary interaction and hopping in the central region. Below we shall apply the theory to two special cases for demonstrations.

(1) *a single quantum dot with multiple levels.* Consider a single quantum dot (QD) connected to electrodes with finite bias voltages, which can be modelled by the Hamiltonian

$$H_{cent} = \sum_i E_i n_i + U \sum_{i<j} n_i n_j \ , \tag{9}$$

where $n_i \equiv c_i^\dagger c_i$ is the particle number operator. For convenience, the particle occupation bases are numbered as $F = \sum_{i=1}^M N_i^F \cdot 2^{i-1}$ and $|F\rangle \equiv (c_M^\dagger)^{N_M^F} \cdots (c_2^\dagger)^{N_2^F} (c_1^\dagger)^{N_1^F} |0\rangle$. Notice that H_{cent} is already diagonalized in the $\{|F\rangle\}$ bases, and the eigenenergy of $|F\rangle$ is $E_{|F\rangle} = \sum_i E_i N_i^F + U \sum_{i<j} N_i^F N_j^F$. The conservable $|l\rangle \langle l|$ can be written explicitly in the form of $\{c_i\}$ and $\{c_i^\dagger\}$ as $m_M^l \cdots m_2^l m_1^l$ where $m_i^l = n_i$ for $N_i^l = 1$ and $m_i^l = 1 - n_i$ for $N_i^l = 0$. The equations of $\{P_F\}$ are simplified to

$$\sum_{i=1}^M (-1)^{N_i^l} \Gamma_i \left[h_i(E_{|F_1\rangle} - E_{|F_0\rangle}) P_{F_0} - \bar{h}_i(E_{|F_1\rangle} - E_{|F_0\rangle}) P_{F_1} \right] = 0 \ \ (l = 1, 2 \cdots 2^M) \ , \tag{10}$$

where $\Gamma_i \equiv \sum_\beta \Gamma_{\beta i}$, $h_i(\omega) \equiv \sum_\beta \frac{\Gamma_{\beta i}}{\Gamma_i} f_\beta(\omega)$, $\Gamma_{\beta i} \equiv \Gamma_{\beta,ii} = 2\pi D_\beta |v_{\beta i}|^2$, $F_1 = l - N_i^l \cdot 2^{i-1} + 2^{i-1}$, $F_0 = l - N_i^l \cdot 2^{i-1}$, and $\bar{h}_i(\omega) \equiv 1 - h_i(\omega)$. The retarded Green function $\tilde{\mathbf{g}}^r(\omega)$ is obtained as

$$\langle\langle c_i | c_j^\dagger \rangle\rangle_0^r = \delta_{ij} \sum_F \frac{P_F}{\omega - \tilde{E}_i^F + \mathrm{i}0^+} \ , \tag{11}$$

with $\tilde{E}_i^F \equiv E_i + U \sum_{j \neq i} N_j^F$ being the renormalized resonances. Specially, for $M = 2$, using $\langle n_1 \rangle = P_{01} + P_{11}$, $\langle n_2 \rangle = P_{10} + P_{11}$, $\langle n_1 n_2 \rangle = P_{11}$, Eq.(19) and Eq.(20) are equivalent to

$$\langle n_i \rangle = (1 - \langle n_{\bar{i}} \rangle) h_i(E_i) + \langle n_{\bar{i}} \rangle h_i(E_i + U) \ , \tag{12}$$

$$\langle n_1 n_2 \rangle = \frac{\Gamma_1}{\Gamma_1 + \Gamma_2} h_1(E_1 + U) \langle n_2 \rangle + \frac{\Gamma_2}{\Gamma_1 + \Gamma_2} h_2(E_2 + U) \langle n_1 \rangle \ , \tag{13}$$

$$\langle\langle c_i | c_i^\dagger \rangle\rangle_0^r = \frac{1 - \langle n_{\bar{i}} \rangle}{\omega - E_i + \mathrm{i}0^+} + \frac{\langle n_{\bar{i}} \rangle}{\omega - E_i - U + \mathrm{i}0^+} \ , \tag{14}$$

with $\bar{i} = 3 - i$ for $i = 1$ or 2. Thus, our theory reproduces the correct results for the occupation number $\langle n_i \rangle$ and the retarded Green function $\langle\langle c_i | c_i^\dagger \rangle\rangle_0^r$ in the limit of $\Gamma_i \to 0$ [3], and derive the correlator $\langle n_1 n_2 \rangle$ which is otherwise difficult to obtain. Fig.1 shows the equilibrium and nonequilibrium distributions for the quantum dot containing two interacting

levels connected with two electrodes. One can see in the plot: (a) The complete Coulomb blockade in equilibrium is partially removed in nonequilibrium, i.e., the blockaded state can be occupied in some "windows" of the gate voltage. (b) The correlator $\langle n_1 n_2 \rangle$ is obviously unequal to $\langle n_1 \rangle \langle n_2 \rangle$ in nonequilibrium, although approximately correct in equilibrium for nondegenerate levels. (c) The total occupation number has fractional steps in nonequilibrium in contrast to integer steps in equilibrium, and the fluctuation of the total number is reminiscent of the shape of tunneling current.

Next, we insert the QD to one arm of a Aharonov-Bohm (AB) interferometer [9]. The other arm (reference arm) is modelled by a quantum point contact, which can be described by adding the term $\sum_k (W e^{\mathrm{i}\phi} a^\dagger_{Lk} a_{Rk} + H.c.)$ to H_T [10], with ϕ being the AB phase induced by magnetic flux. Both the current formula and the equation of $\{P_n\}$ should be modified to include the "direct" coupling between electrodes, the details will be presented elsewhere. The background conductance of the reference arm (measured when QD is decoupled from both electrodes) is $G_0 = \frac{e^2}{h} \frac{4x}{(1+x)^2}$ with $x \equiv \pi^2 W^2 D_L D_R$. The effective conductance of QD is formally defined as $G_{dot} = I(V_b, V_g)/V_b - G_0$. Fig.2 shows the curves of G_{dot} in both linear and nonlinear transport regimes. Three features are noteworthy: (a) In linear transport, the conductance is contributed only by the ground state, while in nonlinear transport, the conductance is contributed by both ground and excited states, recognized by the substeps in the conductance plateaus and valleys, which is in agreement with the recent experiment [11]. (b) With the increase of the background conductance, G_{dot} vs V_g curves exhibit Fano pattern, evolving from a peak (plateau) to a pair of peak and dip (plateau and valley), and finally to a dip (valley), which is originated from the constructive and destructive interference between a resonance and the uniform background. (c) The phase analysis shows that the dependence of G_{dot} on ϕ across a resonance is quite different between linear and nonlinear transport. In linear transport, the dependence changes from $\cos\phi$ to $\cos(\phi + \pi)$ abruptly across a resonance, and $\cos(2\phi)$ component only appears on the resonance. In nonlinear transport, $\cos(2\phi)$ component is always accompanied with the $\cos\phi$ component, and the crossover from $\cos\phi$ to $\cos(\phi + \pi)$ occurs continuously. The "nonequilibrium-Fano" effect discussed here and the "Kondo-Fano" effect in [10] seem to share some similarities, although the mechanisms are basically different.

(2) *coupled double quantum dots.* Consider two quantum dots coupled in series with left and right electrodes (N-QD=QD-N), each dot is capacitively coupled to a gate so that the energy level of the dot is tunable [12]. The coupled double quantum dots can be modelled

by a 4-site Hamiltonian

$$H_{cent} = \sum_{i=1,2}\sum_{\sigma} E_{i\sigma} n_{i\sigma} + t\sum_{\sigma}(c^{\dagger}_{1\sigma}c_{2\sigma} + c^{\dagger}_{2\sigma}c_{1\sigma}) + \sum_{i=1,2} U_i n_{i_\uparrow} n_{i_\downarrow} + U_{12}(n_{1\uparrow}+n_{1\downarrow})(n_{2\uparrow}+n_{2\downarrow}) \quad . \tag{15}$$

We first diagonalize H_{cent} in the 2^4 particle occupation bases. Due to the particle number conservation and spin conservation, the 16 dimensional spaces can be divided into several subspaces $16 = 1 + (2+2) + (1+1+4) + (2+2) + 1$, in which eigenstates are readily solved. In principle, one can find out 2^4 conservables written in $\{c_{i\sigma}\}$ and $\{c^{\dagger}_{i\sigma}\}$ as done in (1), although it is uneasy and unnecessary. We only need to calculate the effective coupling strength $\tilde{\Gamma}^{\beta}_{nm}$ and put them into Eq.(8). With $\{P_n\}$ solved from the 2^4 linear equations, $\tilde{\mathbf{g}}^r$, hence $\mathbf{G}^r$ and $\mathbf{G}^<$ are available. Finally, the current formula in the N-QD=QD-N system can be simplified as

$$I \equiv I_L = -I_R = \sum_{\sigma}\int \frac{d\omega}{2\pi}\Gamma_L\Gamma_R \left|\langle\langle c_{1\sigma}|c^{\dagger}_{2\sigma}\rangle\rangle^r\right|^2 [f_L(\omega) - f_R(\omega)] \quad . \tag{16}$$

We present the numerical results of the tunneling current I vs the resonant levels (E_1, E_2) in Fig.3. The bias voltage V_b ($V_L = V_b/2$, $V_R = -V_b/2$) is fixed as 0.001, 0.3, and 0.6 for the graphs from top to bottom. The graph of $V_b = 0.001$ is corresponding to the linear response regime, in which the thermal distribution in the central region is nearly equilibrium. Due to the intradot and interdot Coulomb interactions, the conductance peaks are arranged to a hexagon pattern, consistent with both experiment and the semiclassical Coulomb blockade model. The graph of $V_b = 0.6$ is corresponding to the strong nonequilibrium case, in which thermal distribution of the central region is determined by two reservoirs with different chemical potentials. The effect of finite bias voltage on the tunneling current is two folded: (a) Pull each conductance peak along the direction of $E_1 = E_2$, and ultimately emerge them into a ridge. It is easy to understand the pulling effect by thinking of the noninteracting case (i.e., $U_1 = U_2 = U_{12} = 0$), where the conductance through N-QD=QD-N is allowed only when $V_L > E_1 \approx E_2 > V_R$. (b) Modify the hexagon pattern significantly, and break the symmetry with respect to $E_1 = E_2$. This can be attributed to the nonequilibrium occupation of the coupled quantum dots. To proceed, let us cut off the interdot hopping for a moment (i.e., $t = 0$). Then the electron filling to the left (right) dot is only related to the chemical potential of the left (right) electrode. The occupation configuration $\{\langle n_1\rangle, \langle n_2\rangle\}$ vs the energy levels (E_1, E_2) has the same shape of hexagon boundary as in the equilibrium case,

except for a displacement of $(\frac{V_b}{2}, -\frac{V_b}{2})$. Therefore, the symmetry with respect to $E_1 = E_2$ is broken when $V_b \neq 0$. Turning on the interdot hopping will make the problem much more complicated, either $\langle n_1 \rangle$ or $\langle n_2 \rangle$ are not good quantum number, energy levels of each dot are hybridized into "molecular orbits", and the occupation of the "molecule" is affected by both of the electrodes. Simple interpretation for this situation is beyond our intelligence.

In conclusion, we have presented a theory dealing with nonequilibrium coherent transport through an arbitrary mesoscopic region, possibly containing strong Coulomb interactions. The only restriction of the theory is that the coupling between the central region and electrodes should be sufficient weak so that the central region may be regarded as a single quantum system. The key innovation of the theory is Eq.(8) which determines the nonequilibrium distribution in an interacting system. The general theory is applied to two special cases, a single quantum dot with multiple interacting levels and coupled double quantum dots, and novel behaviors are found in the nonlinear coherent transport.

We would like to thank W. Li and Y. F. Yang for the valuable discussions. This project was supported by NSFC under Grant No. 10074001 and by the State Key Laboratory for Mesoscopic Physics in Peking University.

* To whom correspondence should be addressed.

REFERENCES

[1] Y. Meir and N. S. Wingreen, Phys. Rev. Lett. **68,** 2512 (1992).

[2] N. E. Bickers, Rev. Mod. Phys. **59,** 845 (1987).

[3] Y. Meir, N. S. Wingreen, and P. A. Lee, Phys. Rev. Lett. **66,** 3048 (1991).

[4] A. L. Yeyati, F. Flores, and A. Martin-Rodero, Phys. Rev. Lett. **83,** 600 (1999).

[5] T. -K. Ng, Phys. Rev. Lett. **76,** 487 (1996).]

[6] J. M. Kinaret *et al.*, Phys. Rev. B **45,** 9489 (1992).

[7] G. Chen, G. Klimeck, and S. Datta Phys. Rev. B **50,** 8035 (1994).

[8] We are only aware of the paper by C. A. Stafford, Phys. Rev. Lett. **77,** 2770 (1996), which is devoted to the identical problem. However, his theory requires the ground state to be nondegenerate, the temperature and the bias voltages are small compared to the excitation energy, while our theory release these restrictions, and is a *real* nonequilibrium transport theory.

[9] A. Yacoby *et al.*, Phys. Rev. Lett. **74,** 4047 (1995).

[10] W. Hofstetter, J. König, and H. Schoeller, Phys. Rev. Lett. **87,** 156803 (2001).

[11] M. M. Deshmukh *et al.*, Phys. Rev. B **65,** 073301 (2002).

[12] F. R. Waugh *et al.*, Phys. Rev. Lett. **75,** 705 (1995); C. Livermore *et al.*, Science **274,** 1332 (1996).

FIGURE CAPTIONS

Fig. 1 Equilibrium and nonequilibrium distributions in a QD containing two energy levels indexed by $i = 1, 2$, connected with two electrodes indexed by $\beta = L, R$. (a), (b) and (c) show the curves of $\langle n_1 \rangle$ (solid) and $\langle n_2 \rangle$ (dotted), $\langle n_1 n_2 \rangle$ (solid) and $\langle n_1 \rangle \langle n_2 \rangle$ (dotted), $\langle n \rangle \equiv \langle n_1 \rangle + \langle n_2 \rangle$ (solid) and $\langle \delta n \rangle \equiv 4 \left[\langle n^2 \rangle - \langle n \rangle^2 \right]^{1/2}$ (dotted) vs the gate voltage V_g, respectively. The bias voltage $V_b \equiv V_L - V_R$ is fixed at $V_b = 0$ / $V_b = 0.6$ for the left / right panel. Other parameters are: $U = 1$, $k_B T = 0.02$, $\Gamma_{1L} = \Gamma_{1R} = \Gamma_{2L} = \Gamma_{2R} = 0.001$, $E_1 = V_g - 0.05$, $E_2 = V_g + 0.05$.

Fig. 2 Linear and nonlinear transport through an AB interferometer embedded with a QD (schematically shown in the inset). (a) and (b) show the curves of $G_{dot} \equiv I(V_b, V_g)/V_b - G_0$ vs the gate voltage V_g for $\phi = 0$, with the bias voltage V_b fixed at 0^+ and 0.6, respectively. The solid, dash, and dotted curves correspond to the background conductance of the reference arm $G_0 = 0$, $0.5\frac{e^2}{h}$, $\frac{e^2}{h}$, respectively. The QD contains three interacting levels, with level spacing $\Delta E = 0.1$, interacting constant $U = 1$, and $\Gamma_L = \Gamma_R = 0.001 \ll k_B T = 0.02$. (c) and (d) analyze the phase dependence of the G_{dot} at the points marked in (a) and (b). Only the range of $0 < \phi < \pi$ is shown since $G_{dot}(\phi) = G_{dot}(-\phi)$.

Fig. 3 Surface graphs of tunneling current I vs the resonant levels (E_1, E_2) in the N-QD=QD-N system, with sideview on the left and topview on the right. The bias voltage is fixed at $V_b = 0.001$, 0.3, and 0.6 for the graphs from top to bottom. Other parameters are: $U_1 = U_2 = 1$, $U_{12} = 0.3$, $t = 0.1$, $k_B T = 0.05$, $\Gamma_L = \Gamma_R = 0.01$. (In the e-print version, Fig. 3 is separated into Fig. 3a, Fig.3b and Fig. 3c corresponding to $V_b = 0.001$, 0.3 and 0.6 respectively, to reduce the size of figures.)

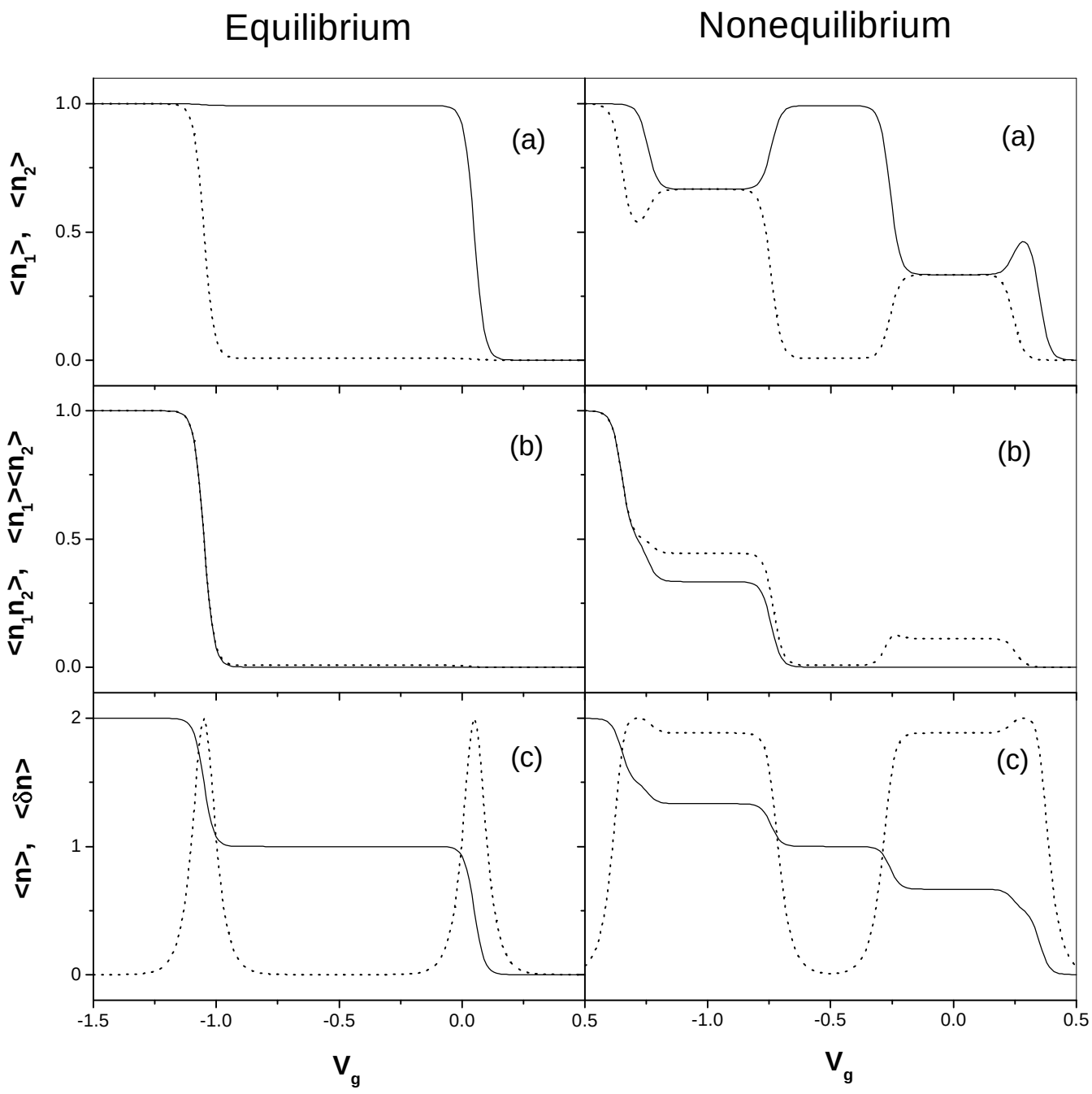
Equilibrium
Nonequilibrium
(a)
(b)
(c)
<n1>, <n2>
<n1n2>, <n1><n2>
<n>, <δn>
1.0
0.5
0.0
2
1
0
-1.5
-1.0
-0.5
0.0
0.5
Vg

Fig.1

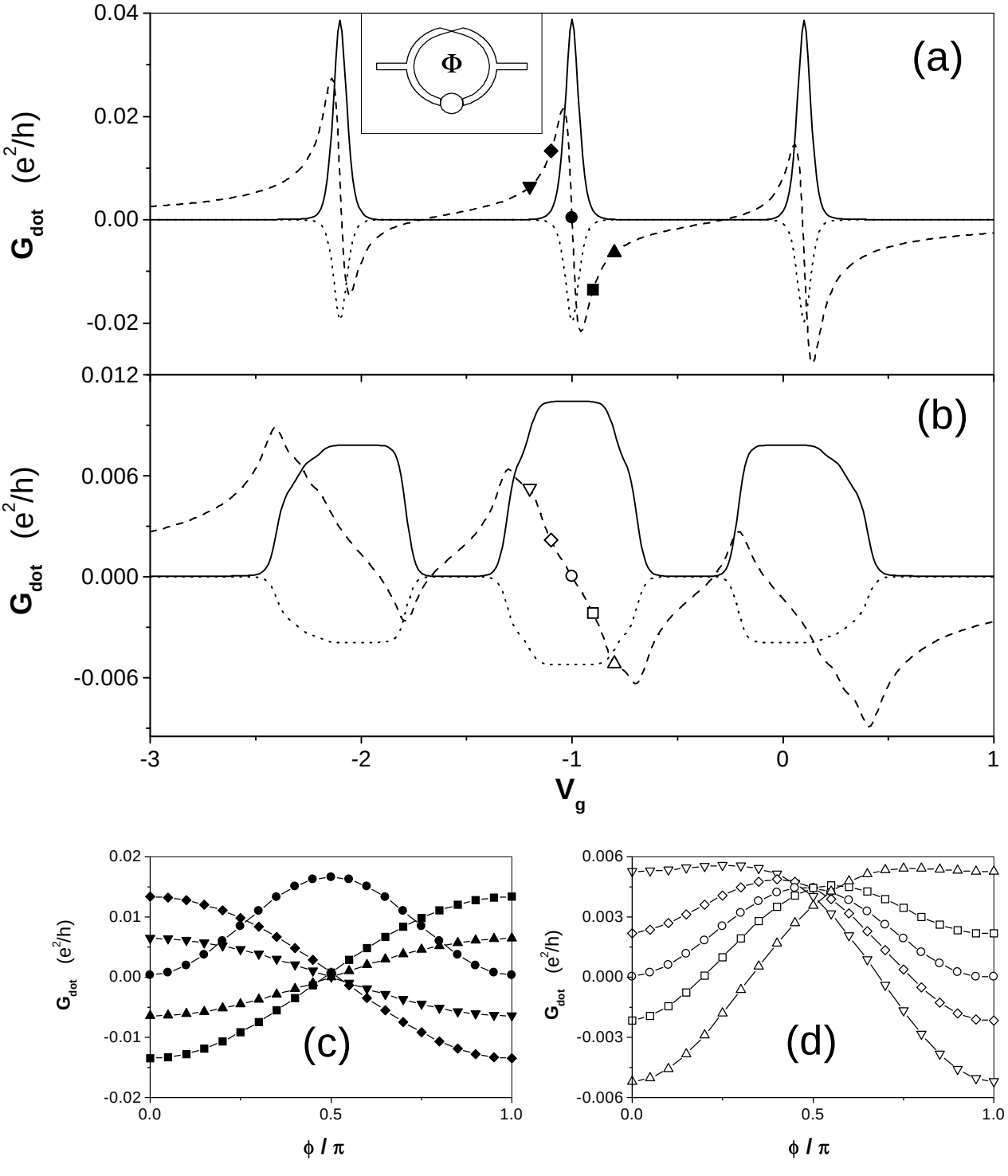

Fig.2

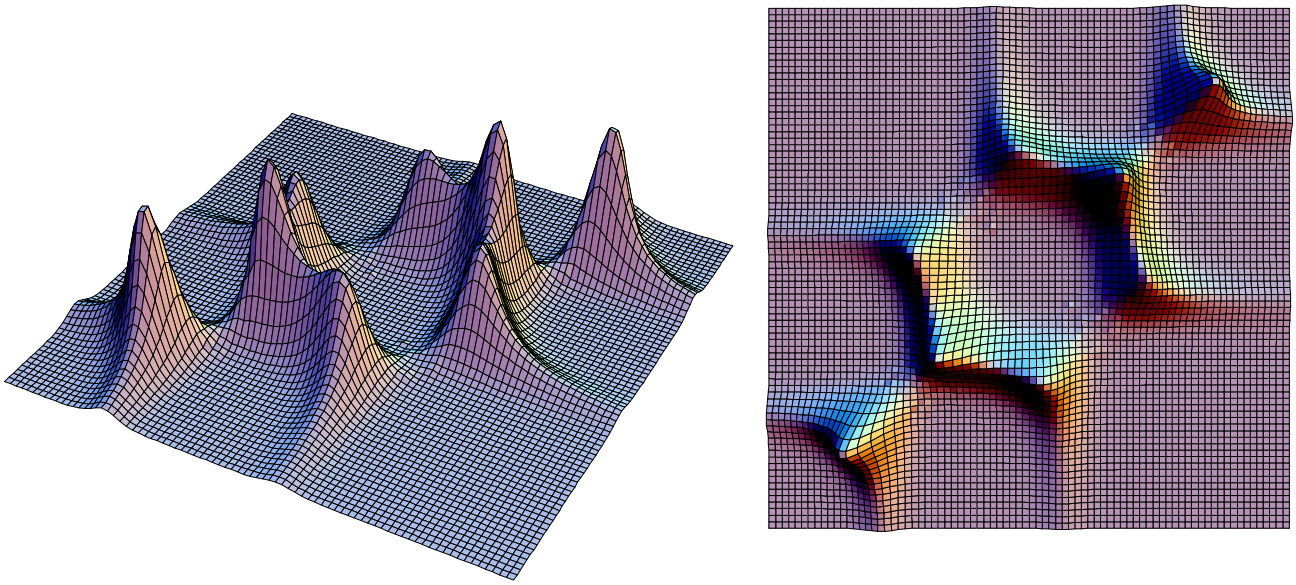

Fig .3 a

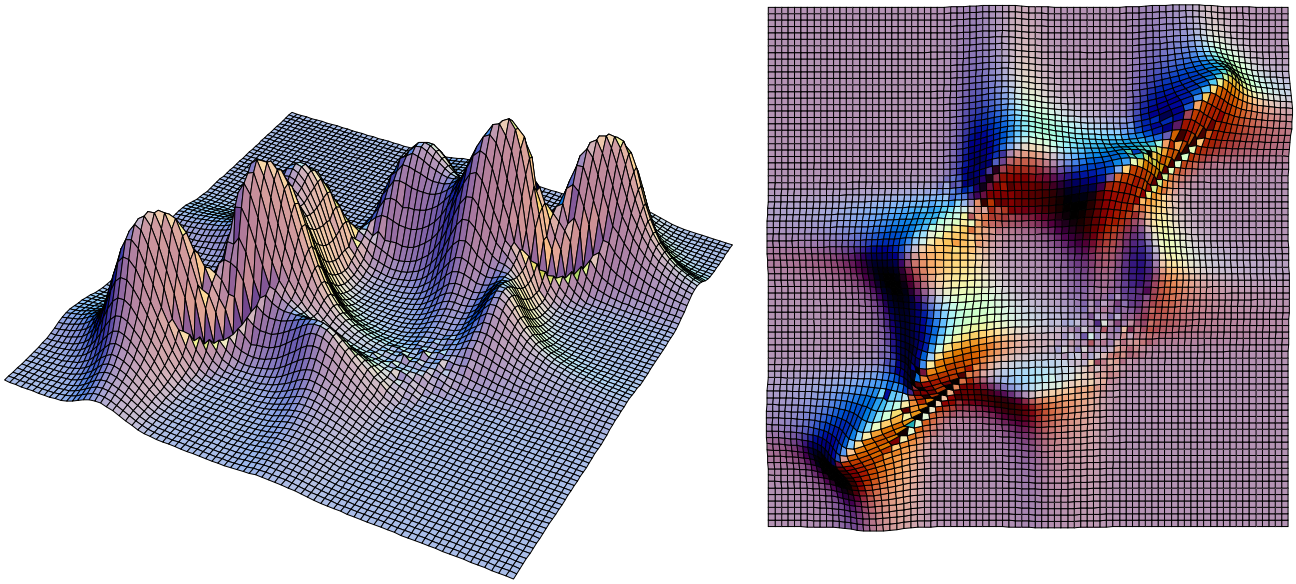

Fig .3 b

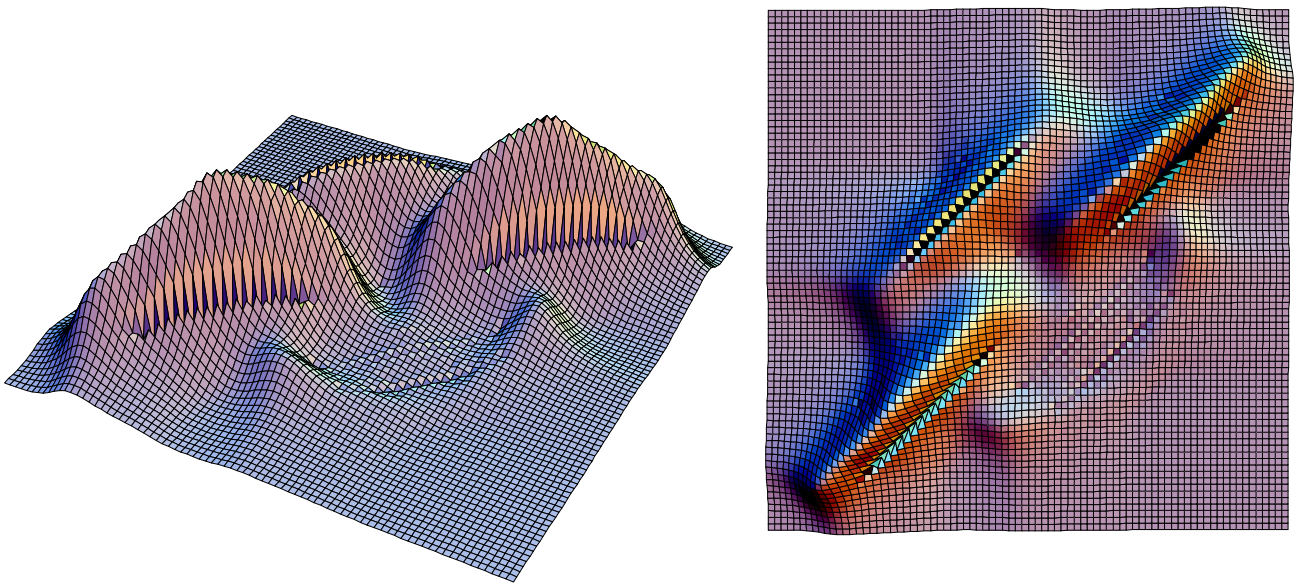

Fig .3 c